

Comparative Studies for the Effect of Dual- and Mono-Organic Modifiers on the Physical Properties of Polyimide-Clay Nanocomposite Membranes

Mei-Chun Lai,¹ Guang-Way Jang,² Kung-Chin Chang,¹ Sheng-Chieh Hsu,¹ Ming-Fa Hsieh,³ Jui-Ming Yeh¹

¹Department of Chemistry, Center for Nanotechnology at CYCU and R & D Center for Membrane Technology, Chung-Yuan Christian University, Chung Li, Taiwan 32023, Republic of China

²Material and Chemical Research Laboratories, Industrial Technology Research Institute, Hsinchu, Taiwan 300, Republic of China

³Department of Biomedical Engineering and Center for Nanotechnology at CYCU Chung-Yuan Christian University, Chung Li, Taiwan 32023, Republic of China

Received 13 August 2007; accepted 28 November 2007

DOI 10.1002/app.27830

Published online 28 April 2008 in Wiley InterScience (www.interscience.wiley.com).

ABSTRACT: In this study, a series of nanocomposite membranes consisted of organic polyimide and organo-modified clay were successfully prepared by an *in situ* polymerization through thermal imidization reactions using a dual- (i.e., CTAB/melamine) and mono-organic modifier as swelling agent of clay mineral. A sequential comparative study was performed to investigate the effect of various feeding ratios of dual- and mono-organic modifiers on the physical properties of as-prepared samples. The as-synthesized nanocomposite membranes were subsequently characterized by WAXRD and TEM. It should be noted that all the nanocomposite membranes prepared from a dual-organic modifier system exhib-

ited a better dispersion of silicate layers in PI matrices as compared with that of mono-organic modifier system. Comparative studies for the effect of various feeding ratios of dual- and mono-organic modifiers on the thermal stability, mechanical strength, molecular barrier properties, and optical clarity of PI-clay nanocomposite membranes were performed with measurements of TGA, DSC, DMA, GPA, VPA, and UV-visible transmission spectroscopy, respectively. © 2008 Wiley Periodicals, Inc. *J Appl Polym Sci* 109: 1730–1737, 2008

Key words: organoclay; polyimides; nanocomposites; membranes

INTRODUCTION

Polymer-clay nanocomposites have received significant attention, since the first report of polyamide-6-clay nanocomposites by Toyota's research group in 1990.^{1–3} Subsequent studies have discovered that physical and chemical properties of organic polymers, such as thermal stability,⁴ mechanical strength,^{3,5,6} solvent resistance,⁷ flame retardation,⁸ ionic conductivity,⁹ corrosion resistance,^{10,11} gas barrier properties,^{12,13} and dielectric properties^{14–16} are substantially improved by the introduction of small portions of inorganic clay. Performance of polymer-clay nanocomposites strongly depends on dispersion and spacing between clay layers. According to the distance between layers, the polymer-clay nanocomposites can be divided into two categories: intercalated and exfo-

liated.^{17,18} The enhancements of physical and chemical properties occur even with the addition of low percentages of organically modified clay; the properties are maximized when the clay platelets are exfoliated and randomly dispersed in a polymer matrix.

Aromatic polyimide (PI) is well known as a high-temperature engineering polymer. Compared with most organic polymeric materials, PI exhibits superior thermal stability and mechanical strength. Attempts are being made to use the materials for fabrication of high performance components and devices.^{19,20} PI-clay nanocomposite membranes derived from poly(amic acid) (PAA) and clay have been described by Yano et al.^{12,21} and Lan et al.⁴ The resulting PI-clay nanocomposite membranes display improved gas barrier properties and reduced thermal expansion coefficient (CTE). An organic modifier is typically used to extend spacing between silicate layers for intercalation of matrix polymers. Organic modifiers also serve as compatibilizers for inorganic clay and organic polymer. Ionic interaction is limited to organic modifiers and silicate sheets. A stronger interaction or even a bond between organic and inorganic moieties would further improve performance of hybrid materials.

Correspondence to: J.-M. Yeh (juiming@cycu.edu.tw).

Contract grant sponsor: the Center-of-Excellence Program on Membrane Technology, the Ministry of Education, Taiwan, Republic of China; contract grant number: NSC 94-2113M-033-008.

In this study, we present a sequential comparative study for the effect of dual- and mono-organic modifier as swelling agent of clay mineral on the PI-clay nanocomposite membranes. In this dual-organic modifier system, we envisioned that the bonding between organic and inorganic moieties is achieved by subsequent usage of a long chain modifier and a short chain multi-functional modifier for the treatment of clay. Intercalation of cationic exchanged montmorillonite (MMT) clay using hexadecyltrimethylammonium bromide (CTAB) and/or melamine alone have also been investigated for comparative studies. The as-synthesized nanocomposite membranes were subsequently characterized by wide-angle X-ray diffraction (WAXRD) and transmission electron microscopy (TEM). Comparative studies for the effect of various feeding ratios of dual- and mono-organic modifiers on the thermal stability, mechanical strength, molecular barrier properties, and optical clarity of PI-clay nanocomposite membranes were performed with the measurements of thermal gravimetric analysis (TGA), differential scanning calorimetry (DSC), dynamic mechanical analysis (DMA), gas permeability analysis (GPA), vapor permeability analyzer (VPA), and UV-visible transmission spectroscopy, respectively.

EXPERIMENTAL

Materials

The MMT clay, consisted of a unit cell formula $\text{Na}_{0.31}[\text{Al}_{1.67}\text{Mg}_{0.33}]\text{Si}_4\text{O}_{10}(\text{OH})_2 \cdot \dots \cdot 7.5\text{H}_2\text{O}$ and a cation exchange capacity (CEC) of 116 mEq/100 g, was supplied by Pai-Kong ceramic company, Taiwan. Hexadecyltrimethylammonium bromide (Sigma, 97.0%, referred as CTAB) and melamine (Lancaster, 99.0%), as denoted in Figure 1, were used as swelling agents. Precursors for the synthesis of PI, such as 4,4'-Oxydianiline (97.0%, referred as ODA) and 4,4'-(4,4'-Isopropylidenediphenoxy)-bis(phthalic anhydride) (97.0%, referred as BASS) were purchased from Aldrich Chemical. *N,N*-Dimethylacetamide (Riedel-de Haen, 99.0%, referred as DMAc) and hydrochloric acid (Riedel-de Haen, 37%) were used as received.

Preparation of CTAB/melamine modified clay with various CTAB/melamine ratios

The organic modified clay was prepared by cationic exchange sodium ions in MMT clay with alkyl ammonium ions of swelling agents. The molar ratios of CTAB/melamine are 1.2/0, 0.6/0.6, 0.4/0.8, 0.8/0.4 or 0/1.2 (it should be noted that the molar ratio of CTAB/melamine = 1.2/0 and 0/1.2 represented the mono-organic modifier system). Typically, 5 g of

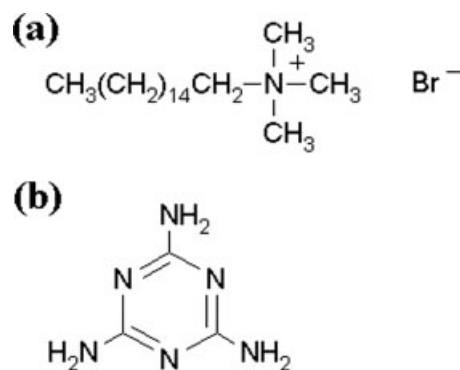


Figure 1 (a) Chemical structure of organophilic MMT CTAB, (b) Chemical structure of organophilic MMT Melamine.

MMT clay with CEC value of 116 mequiv/100 g was stirred in 600 mL of distilled water (beaker A) at room temperature overnight. Separated solutions containing different concentrations of CTAB, 2.54 g (1.2), 1.27 g (0.6), 0.85 g (0.4) or 1.69 g (0.8), in another 30 mL of distilled water (beaker B) were prepared by magnetic stirring, followed by the addition of 1.0M HCl aqueous solution to adjust the pH value to 3–4. After stirring for 3 h, the protonated amino acid solution (beaker B) was added at a rate of approximately 10 mL/min with vigorous stirring to the clay suspension (beaker A). The mixture was stirred overnight at room temperature. Then, solutions containing different concentration of melamine, 0.44 g (0.6), 0.29 g (0.4), 0.59 g (0.8) or 0.88 g (1.2), in 30 mL of distilled water (beaker C) were prepared by the same procedure as that for CTAB solution but adding 15 mL of 1.0M HCl instead. After stirring for 3 h, the protonated melamine solution (beaker C) was added to the Clay/CTAB mixture (beaker A+B) at a rate of approximately 10 mL/min with vigorous stirring. The mixture was again stirred overnight at room temperature. The organic modified clay was recovered by ultracentrifuging (9000 rpm, 30 min) and filtering the solution in a Buchner funnel. Purification of products was performed by washing and filtering samples repeatedly (at least four times each) to remove sodium chloride and any excess of ammonium ions.

Synthesis of polyimide and polyimide-clay nanocomposite membranes by thermal imidization

PI and PI-clay nanocomposite membranes were prepared by thermal imidization that can be found elsewhere.¹¹

Characterization of nanocomposite membranes

Structures of a nanocomposites and the nature of polymer-clay interaction can be better illustrated

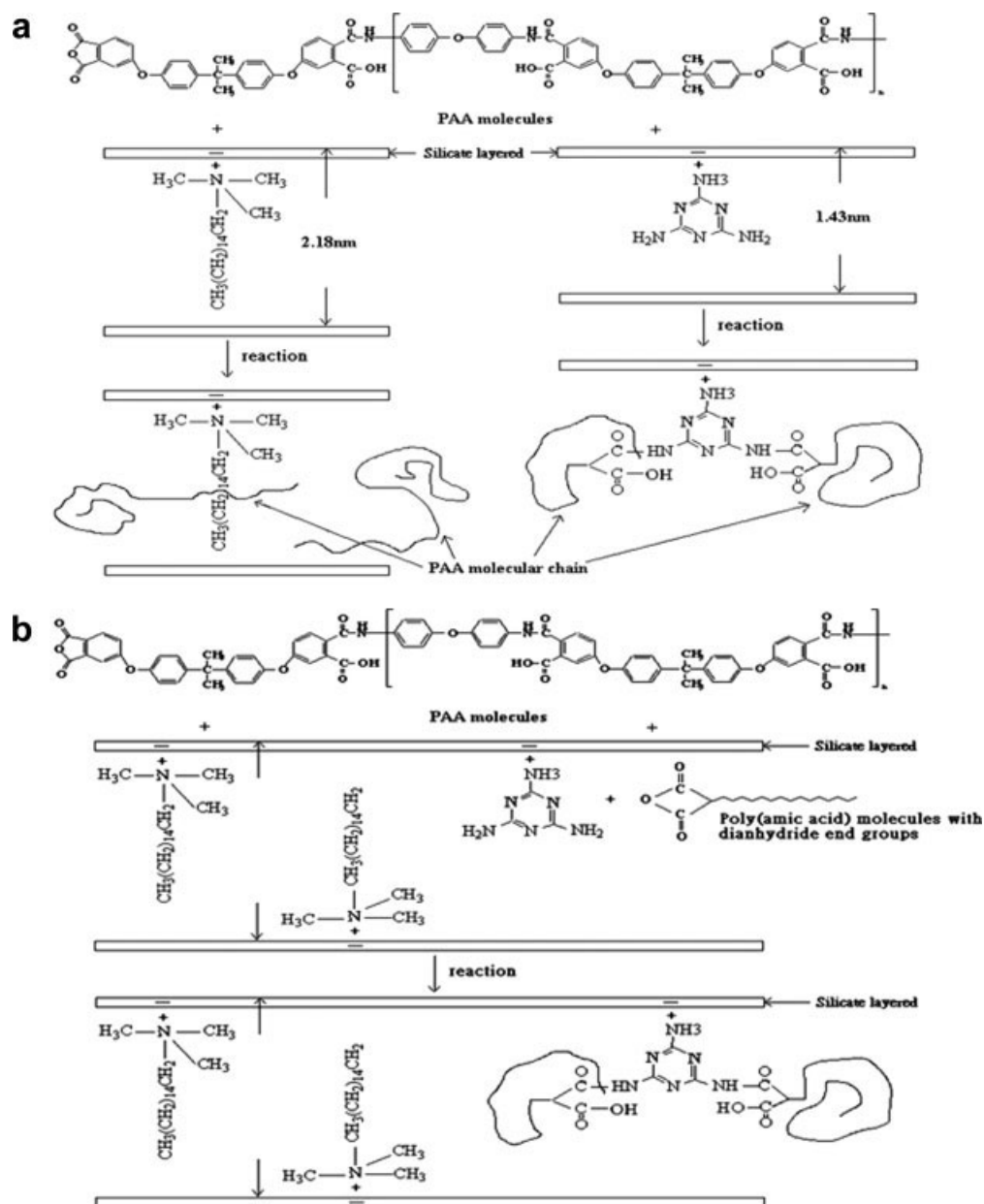


Figure 2 Schematic drawing of (a) mono- or (b) dual-swelling-agent (CTAB/Melamine = 1.2/0, 0.6/0.6, 0.4/0.8, 0.8/0.4, 0/1.2) for intercalating layered silicates and reacting with PAA molecules.

based on X-ray diffraction (XRD) measurement of d spacing of a clay and TEM image of clay layers in polymer matrix. WAXRD studies were performed on a Rigaku D/MAX-3C OD-2988N X-ray diffractometer with copper target and Ni filter at a scanning rate of $2^\circ/\text{min}$. The samples for TEM study were first prepared by putting the membrane of PI/clay nanocomposite materials into epoxy resin capsules followed by curing the epoxy resin at 100°C for 24 h in a vacuum oven. Then the cured epoxy resin containing PI/clay nanocomposite materials were microtome with Reichert-Jung Ultracut-E into 60–90 nm-thick slices. Subsequently, a layer of carbon about 10 nm thick was deposited on these slices on mesh 300 cop-

per nets for TEM observations on a JEOL-200FX with an acceleration voltage of 120 kV.

TGA and DSC were employed to record the thermal properties of specimens. TGA scans were performed on a DuPont TA Q50 thermal analysis system in a nitrogen atmosphere. The scan rate was $20^\circ\text{C}/\text{min}$, and temperature range was from 40 to 900°C . DSC was performed on a DuPont TA Q10 differential scanning calorimeter at a heating or cooling rate of $10^\circ\text{C}/\text{min}$ in nitrogen atmosphere. The temperature range was from 25 to 350°C . The glass transition temperature (T_g) of PI and PCN membranes was recorded based on the second scanning. The DMA of the PI/clay nanocomposite membranes

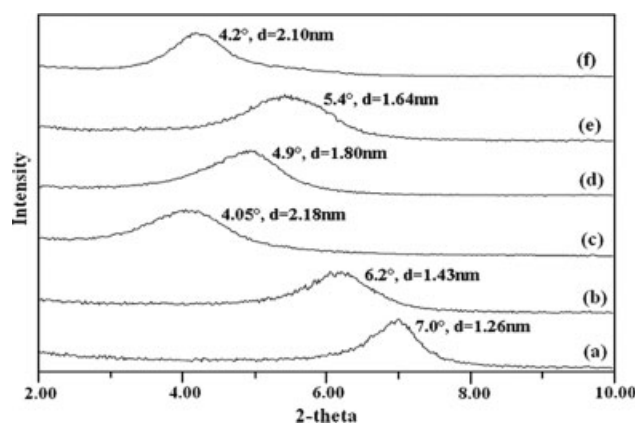


Figure 3 Wide-angle powder XRD patterns of (a) pristine clay; (b)-(f) clay-(CTAB/Melamine = 0/1.2, 1.2/0, 0.6/0.6, 0.4/0.8, 0.8/0.4).

were performed from 30 to 350°C with a DuPont TAQ800 analyzer at a heating rate of 3°C/min and at a frequency of 1 Hz. A model GTR 10 gas permeability analyzer (Yanagimoto Co., Kyoto, Japan) was used to carry out the permeation experiment of oxygen gas and water vapor. UV-visible transmission spectra were obtained using a Hitachi U-2000 UV-visible spectrometer.

Preparation of membranes and barrier property measurements

The membranes of as-prepared PI or PI-clay nanocomposite materials were prepared for the measurements of the molecular (O_2 and H_2O) barrier property that had been reported in our earlier literatures.¹¹

RESULTS AND DISCUSSION

The schematic drawings of a reaction between dual- or mono-swelling-agent modified silicates and PAA are presented in Figure 2. For the mono-organic modified system [Fig. 2(a)], a $(CH_3)_3N^+$ group of long chain swelling agent (CTAB) forms an ionic bond with negatively charged silicate layers by replacing Na^+ . The long chain swelling agent also opens silicate layer galleries for PAA insertion. For a short chain swelling agent (melamine) containing three amine ($-NH_2$) groups, all NH_2 end groups could interact with negatively charged silicate layers. However, only a very small amount of excess $-NH_2$ can react with the dianhydride end group in PAA. However, for the dual-modifier system [Fig. 2(b)], a long chain swelling agent was first introduced to open silicate layers galleries for subsequent intercalation of a multi-functional swelling agent. Reaction of remaining $-NH_2$ of melamine and dianhydride end group in PAA results in a greater

interaction force due to the formation of chemical bonds. Silicate layers can be pushed apart further to achieve intercalation or exfoliation structures.

Structure of PI-clay nanocomposite membranes

Wide-angle powder XRD patterns between $2\theta = 2-10^\circ$ of pristine clay and clay-(CTAB/Melamine) with various CTAB/melamine ratios were recorded and shown in Figure 3. In Figure 3(a), a diffraction peak at $2\theta = 7.0^\circ$, equaling a d_{001} spacing of 1.26 nm, was displayed for the layered silicates of pristine clay. For the mono-organic modified clay, the d_{001} spacing of melamine (0/1.2) and CTAB (1.2/0) intercalated clay specimens are 1.43 and 2.18 nm, as shown in Figure 3(b,c), respectively. Since d_{001} spacing of pristine clay is 1.26 nm, d spacing greater than the number indicate intercalation of melamine and CTAB between layers of clay. The reflection shifts progressively toward a lower angle with increasing CTAB content in the clay-(CTAB/melamine).

Figure 4 presents the WAXRD patterns for PI and PI/clay-(CTAB/melamine) (97/3) nanocomposite membranes with various CTAB/melamine ratios with 2θ angle ranging from 2 to 10° . Figure 4(b) shows a broad peak at $2\theta = 6.0^\circ$ (d_{001} spacing = 1.47 nm). This indicates that melamine chains alone can not effectively promote the insertion of monomers. The d_{001} spacing of the clay interlayer increases progressively with an increase of the CTAB content of dual modifier in the PI-clay nanocomposite membranes. A lack of any diffraction peaks for composites of clay-(CTAB/melamine = 1.2/0, 0.6/0.6, 0.4/0.8, and 0.8/0.4), as shown in Figure 4(c-f), indicates that the d_{001} spacing between the layered silicates has been either intercalated to a distance of more than 4.42 nm ($2\theta < 2.0^\circ$) or exfoliated completely in ODA-BASS.

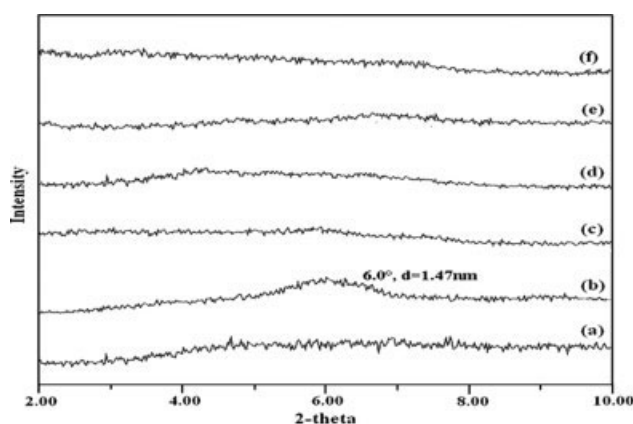


Figure 4 WAXRD patterns ranging from $2\theta = 2-10^\circ$ for (a) pure PI; (b)-(f) PI/clay-(CTAB/Melamine = 0/1.2, 1.2/0, 0.6/0.6, 0.4/0.8, 0.8/0.4) = 97/3.

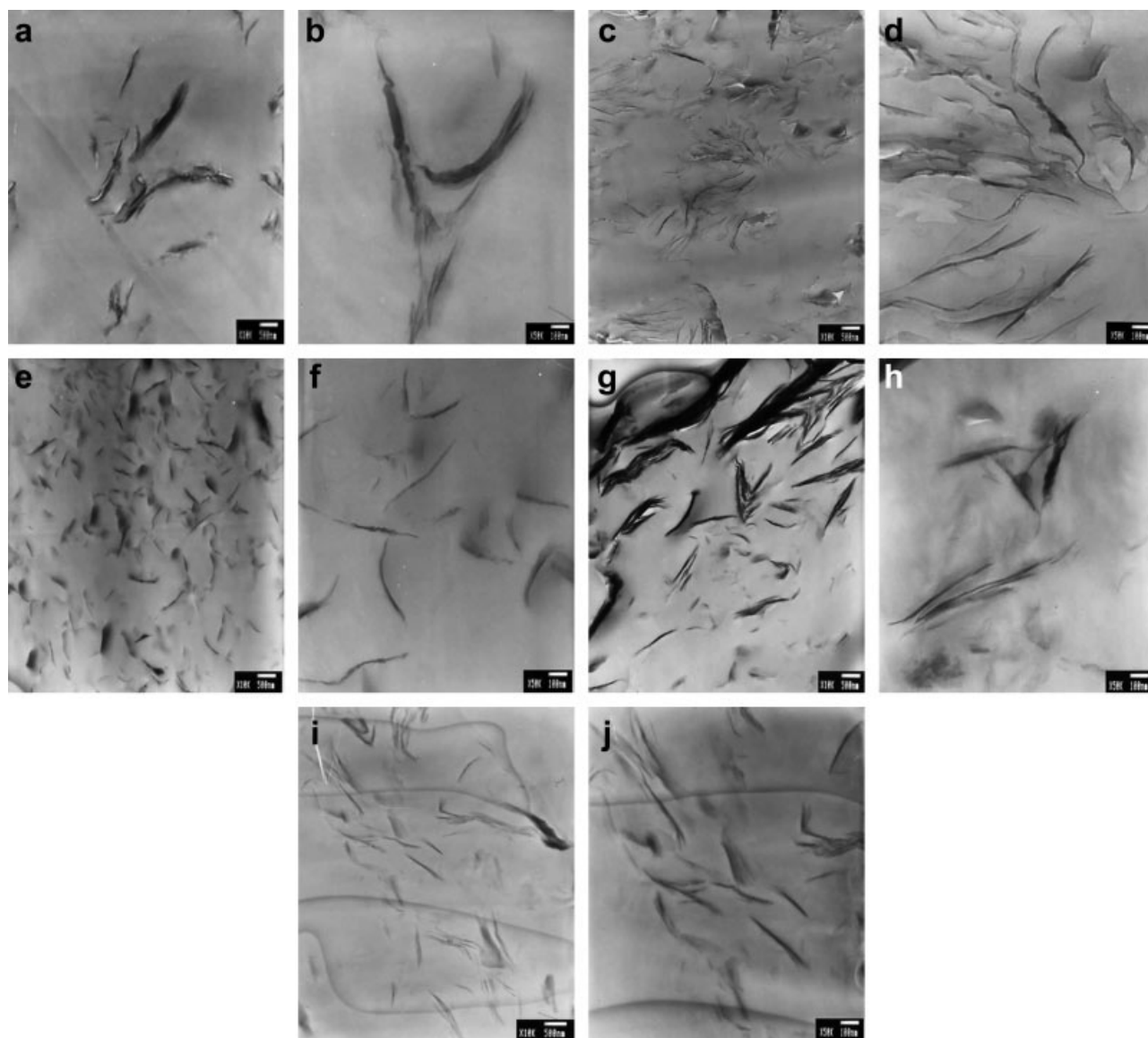


Figure 5 TEM images for different PI/clay nanocomposites containing 3 wt % (a,b) clay-(CTAB/Melamine = 0/1.2); (c,d) clay-(CTAB/Melamine = 1.2/0); (e,f) clay-(CTAB/Melamine = 0.6/0.6); (g,h) clay-(CTAB/Melamine = 0.4/0.8); (i,j) clay-(CTAB/Melamine = 0.8/0.4) at low ($\times 10k$) and high ($\times 50k$) magnification.

Further evidence of this nanometer-scale dispersion of intercalated silicate layers in ODA-BASS can be supported by TEM images. TEM images at low magnification are used to determine if the clay is well-dispersed in the polymer, while the high magnification images enable the description as intercalated or exfoliated. Five cases of PI that containing 3 wt % clay-(CTAB/melamine) with various CTAB/melamine ratios were chosen for comparison, and their TEM images are shown in Figure 5(a–j). The light regions represent PI, and the dark lines correspond to the silicate layers. For PI-clay nanocomposite membranes containing 3 wt % clay-(CTAB/Melamine = 0.6/0.6), as shown in Figure 5(e–f), isolated and exfoliated structures were observed. On the

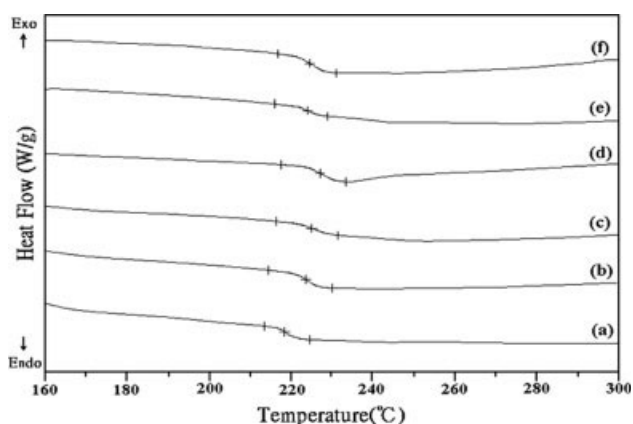


Figure 6 DSC curves of (a) pure PI; (b–f) PI/clay-(CTAB/Melamine = 0/1.2, 1.2/0, 0.6/0.6, 0.4/0.8, 0.8/0.4) = 97/3.

TABLE I
Relations of Composition of PI-Clay Nanocomposite Membranes to Thermal, Mechanical, and Barrier Properties Measured by TGA, DSC, DMA, GPA, and VPA

Compound code	Feed composition (wt %)		Thermal properties (°C)			Mechanical properties (MPa) E'	Barrier properties	
	PI	MMT	T_d	T_g	T_g		(Barrer) O ₂	(g/m ² h) H ₂ O
Pure PI (ODA-BASS)	100	0	514.3	218.5	238.8	2289	0.2896 ± 0.025	108.4 ± 6.3
PI/clay-(CTAB/Melamine = 0/1.2)	97.00	3.00	518.8	223.5	245.4	2634	0.2196 ± 0.020	85.3 ± 4.2
	95.00	5.00	523.2	226.7	248.8	2966	0.1984 ± 0.012	63.5 ± 3.7
PI/clay-(CTAB/Melamine = 1.2/0)	97.00	3.00	522.8	225.0	250.7	3207	0.2126 ± 0.016	69.4 ± 2.2
	95.00	5.00	530.2	229.1	253.2	3510	0.1880 ± 0.010	49.3 ± 2.2
PI/clay-(CTAB/Melamine = 0.6/0.6)	97.00	3.00	526.3	227.2	253.4	3483	0.2080 ± 0.015	66.9 ± 1.3
	95.00	5.00	531.1	230.4	255.6	3737	0.1796 ± 0.009	46.5 ± 1.1
PI/clay-(CTAB/Melamine = 0.4/0.8)	97.00	3.00	520.4	224.1	248.1	3008	0.2173 ± 0.019	84.4 ± 3.4
	95.00	5.00	526.6	227.7	251.0	3295	0.1943 ± 0.012	61.8 ± 3.1
PI/clay-(CTAB/Melamine = 0.8/0.4)	97.00	3.00	521.1	224.7	248.1	3161	0.2144 ± 0.018	70.2 ± 3.0
	95.00	5.00	529.7	228.3	252.3	3443	0.1882 ± 0.010	52.8 ± 2.7

other hand, Figure 5(a,b) appear to be almost entirely intercalated while Figure 5(c,d,g-j) show a combination of both intercalated and exfoliated structures. This suggests that a greater interaction force between PI and organic modifiers are required for formation of exfoliated structures. The difference in the morphology of the PI/clay nanocomposites formed by swelling agents with various ratios of CTAB/melamine, therefore, affects their thermal, mechanical, molecular barrier and optical properties.

Thermal properties of PI-clay nanocomposite materials

Influence of CTAB/melamine ratios on glass transition temperatures (T_g) of PI/clay-(CTAB/melamine) nanocomposites was investigated using DSC and results are shown in Figure 6. Glass transition temperatures of PI and PI/clay-(CTAB/melamine) = 97/3 and 95/5 nanocomposites are listed in Table I. PI/clay-(CTAB/melamine) nanocomposites [Fig. 6(b-f)] showed an increased T_g compared with that of PI [Fig. 6(a)] due to limited mobility of PI within silicate layers. The results indicate that PI-clay nanocomposites with CTAB/melamine ratio of 0.6/0.6 have more profound effect on glass transition temperature of composites. This may due to formation of exfoliated structures in the composites containing 0.6/0.6 ratio of organic modifiers.

Figure 7 shows TGA thermograms for PI and PI/clay-(CTAB/melamine) nanocomposites with various CTAB/melamine ratios. The thermal decomposition temperatures (T_d) were measured at onset point from TGA measurement. The T_d of PI and PI/clay-(CTAB/melamine) = 97/3 and 95/5 nanocomposites are summarized in Table I. Evidently, T_d of PI/clay-(CTAB/melamine) nanocomposites [Fig. 7(b-f)] are significantly higher than that of PI [Fig. 7(a)]. It is observed that the PI/clay-(CTAB/melamine)

nanocomposites possess higher thermal stability when MMT is well dispersed.

Mechanical properties of PI-clay nanocomposite materials

Thermomechanical properties of PI and PI/clay-(CTAB/melamine) nanocomposite membranes with various CTAB/melamine ratios were investigated by means of DMA and results are illustrated in Figure 8 and Table I. A strong interaction between clay and PI matrix limits movement of PI chain segments that results an enhancement in storage modulus of PI in the presence of organic modified clay as shown in Figure 8. Figure 8 and Table I also indicate that PI-clay nanocomposites with CTAB/melamine ratio of 0.6/0.6 have more profound effect on thermomechanical property of composites. This significant enhancement in storage modulus can be attributed to the clay-(CTAB/melamine = 0.6/0.6) resulting in a greater clay-matrix interfacial area. Glass transition

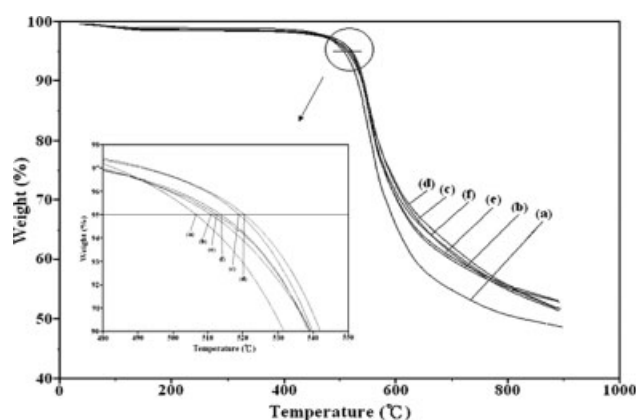


Figure 7 TGA thermograms of weight loss as a function of temperature for (a) pure PI; (b-f) PI/clay-(CTAB/Melamine = 0/1.2, 1.2/0, 0.6/0.6, 0.4/0.8, 0.8/0.4) = 97/3.

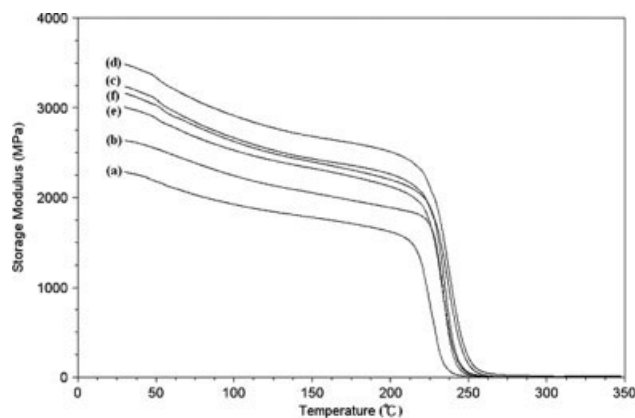


Figure 8 The storage modulus of (a) pure PI; (b–f) PI/clay-(CTAB/Melamine = 0/1.2, 1.2/0, 0.6/0.6, 0.4/0.8, 0.8/0.4) = 97/3.

temperature of PI-clay nanocomposite membranes obtained from $\tan \delta$ are also summarized in Table I. Shift of $\tan \delta$ peak to a higher temperature is consistent with DSC studies.

Oxygen and vapor permeability of PI-clay nanocomposite membranes

Gas and moisture permeability measurements were carried out for PI and PI-clay nanocomposite membranes with thickness of about 90 μm . The analyze data of oxygen and water vapor permeability were measured at least three times. As shown in Figures 9, 10, and Table I, compared with PI film, PI/clay-(CTAB/Melamine) nanocomposite membranes exhibit lower oxygen and water vapor permeability. This is attributed to the plate-like clay layers effectively increase the length of diffusion pathways thus limits permeability of PI/clay-(CTAB/Melamine) nanocomposite membranes. Figures 9, 10, and Table I also designate that PI-clay nanocomposites with

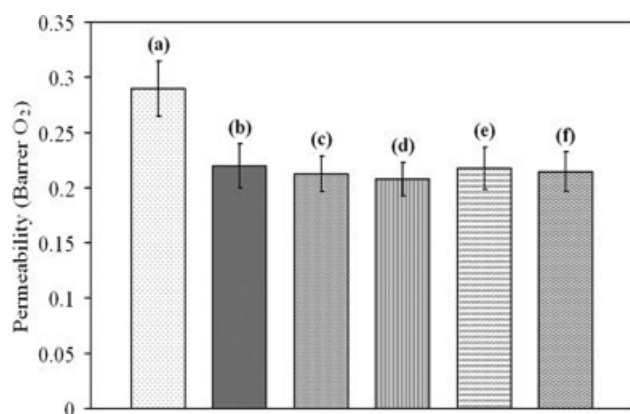


Figure 9 Permeability of O_2 as a function of (a) pure PI; (b–f) PI/clay-(CTAB/Melamine = 0/1.2, 1.2/0, 0.6/0.6, 0.4/0.8, 0.8/0.4) = 97/3.

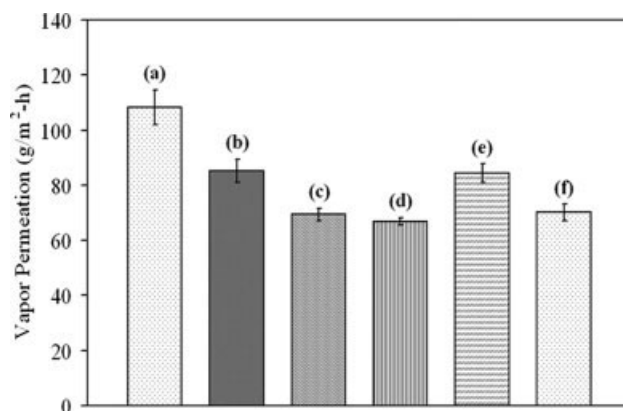


Figure 10 Permeability of H_2O vapor as a function of (a) pure PI; (b–f) PI/clay-(CTAB/Melamine = 0/1.2, 1.2/0, 0.6/0.6, 0.4/0.8, 0.8/0.4) = 97/3.

CTAB/melamine ratio of 0.6/0.6 have more profound effect on molecular barrier property of composites. This enhanced molecular barrier effect could be associated that PI-clay nanocomposites with CTAB/melamine ratio of 0.6/0.6 have better dispersion of clay platelets than PI-clay nanocomposites with other various CTAB/melamine ratios.

Optical clarity of PI-clay nanocomposite membranes

Figure 11 shows UV/visible transmission spectra of PI and PI/clay-(CTAB/melamine) = 97/3 nanocomposite membranes with various CTAB/melamine ratio. Membrane of PI-clay nanocomposites with CTAB/melamine ratio of 0.6/0.6 is the most transparent one. This suggests that layer silicate is better dispersing in PI matrix for PI-clay nanocomposite membranes with CTAB/melamine molar ratio of 0.6/0.6. This is consistent with results WAXRD and TEM studies.

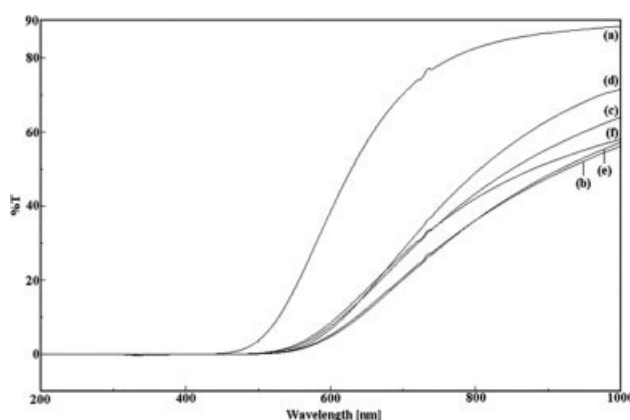


Figure 11 UV/visible transmission spectra of (a) pure PI; (b–f) PI/clay-(CTAB/Melamine = 0/1.2, 1.2/0, 0.6/0.6, 0.4/0.8, 0.8/0.4) = 97/3. Membrane thickness $\sim 90 \mu\text{m}$.

CONCLUSIONS

PI-clay nanocomposite membranes with improved thermal, mechanical, molecular barrier, and optical properties were achieved by using dual-swelling agents as compared with that of mono-organic modifier. The clay was first swelled with a long chain swelling agent, CTAB, to open a channel for intercalation of a short chain reactive swelling agent, melamine. Reaction of melamine and PAA results in increase of d_{001} spacing or exfoliation of clay layers. Effects of various CTAB/melamine ratios of clay-(CTAB/melamine) on formation and properties of intercalated PI nanocomposites were investigated. The as-synthesized PI-clay nanocomposite membranes were characterized by WAXRD and TEM. PI/clay-(CTAB/melamine = 0.6/0.6) nanocomposites showed better dispersion of the clay platelets than PI/clay-(CTAB/Melamine = 0/1.2, 1.2/0, 0.4/0.8, and 0.8/0.4) nanocomposites according to TEM studies.

The PI nanocomposite membranes containing clay-(CTAB/melamine = 0.6/0.6) exhibited better thermal stability, mechanical strength, molecular barrier properties, and optical clarity than PI nanocomposite containing clay-(CTAB/melamine = 0/1.2, 1.2/0, 0.4/0.8, and 0.8/0.4) according to TGA, DSC, DMA, GPA, VPA, and UV-visible transmission spectroscopy. This results confirms that the better dispersibility and increased interfacial adhesion of the clay-(CTAB/melamine = 0.6/0.6) with PI matrix are responsible for physical, mechanical, and molecular barrier properties improvements.

References

1. Usuki, A.; Kawasumi, M.; Kojima, Y.; Okada, A.; Kurauchi, T.; Kamigaito, O. *J Mater Res* 1993, 8, 1174.
2. Usuki, A.; Kojima, Y.; Kawasumi, M.; Okada, A.; Fukushima, Y.; Kurauchi, T.; Kamigaito, O. *J Mater Res* 1993, 8, 1179.
3. Kojima, Y.; Usuki, A.; Kawasumi, M.; Okada, A.; Fukushima, Y.; Kurauchi, T.; Kamigaito, O. *J Mater Res* 1993, 8, 1185.
4. Lan, T.; Kaviratna, P. D.; Pinnavaia, T. *J Chem Mater* 1994, 6, 573.
5. Massersmith, P. B.; Giannelis, E. P. *Chem Mater* 1994, 6, 1719.
6. Tyan, H. L.; Liu, Y. C.; Wei, K. H. T. *Chem Mater* 1999, 11, 1942.
7. Burnside, S. D.; Giannelis, E. P. *Chem Mater* 1995, 7, 1597.
8. Gilman, J. W.; Jackson, C. L.; Morgan, A. B.; Hayyis, R. Jr.; Manias, E.; Giannelis, E. P.; Wuthenow, M.; Hilton, D.; Philips, S. H. *Chem Mater* 2000, 12, 1866.
9. Vaia, R. A.; Vasudevan, S.; Krawiec, W.; Scanlon, L. G.; Giannelis, E. P. *Adv Mater* 1995, 7, 154.
10. Yeh, J. M.; Liou, S. J.; Lin, C. Y.; Wu, P. C.; Tsai, T. Y. *Chem Mater* 2001, 13, 1131.
11. Yu, Y. H.; Yeh, J. M.; Liou, S. J.; Chang, Y. P. *Acta Mater* 2004, 52, 475.
12. Yano, K.; Usuki, A.; Kurauchi, T.; Kamigaito, O. *J Polym Sci Part A: Polym Chem* 1993, 31, 2493.
13. Messersmith, P. B.; Giannelis, E. P. *J Polym Sci Part A: Polym Chem* 1995, 33, 1047.
14. Jiang, L. Y.; Leu, C. M.; Wei, K. H. *Adv Mater* 2002, 14, 426.
15. Zhang, Y. H.; Dang, Z. M.; Fu, S. Y.; Xin, J. H.; Deng, J. G.; Wu, J.; Yang, S.; Li, L. F.; Yan, Q. *Chem Phys Lett* 2005, 401, 553.
16. Wang, H. W.; Dong, R. X.; Chu, H. C.; Chang, K. C.; Lee, W. C. *Mater Chem Phys* 2005, 94, 42.
17. Fan, X.; Xia, C.; Advincula, R. C. *Colloid Surf A: Physicochem Eng Aspects* 2003, 219, 75.
18. Koo, C. M.; Kim, S. O.; Chung, I. J. *Macromolecules* 2003, 36, 2758.
19. Wilson, D.; Stenzenberger, H. D.; Hergenrother, P. M. *Polyimides*; Blackie: London, 1990.
20. Ghost, M. K.; Mittal, K. L.; *Polyimides: Fundamentals and Applications*; Marcel Dekker: New York, 1996.
21. Yano, K.; Usuki, A.; Okada, A. *J Polym Sci Part A: Polym Chem* 1997, 35, 2289.